Supporting Information

Secondary Interaction Interfaces with PCNA Control Conformational Switching of DNA Polymerase PolB from Polymerization to Editing

Xiaojun Xu, Chunli Yan, Bradley R. Kossmann, Ivaylo Ivanov*

Department of Chemistry, Center for Diagnostics and Therapeutics, Georgia State University, Atlanta, Georgia 30302, United States

Corresponding Author
* E-mail: iivanov@gsu.edu. Tel: +1 (404) 413-5529. Fax: +1 (404) 413-5505.

I. Supplementary Figures

II. Supplementary movies

III. Supplementary Tables

IV. Supplementary atomic models

V. References

I. Supplementary Figures

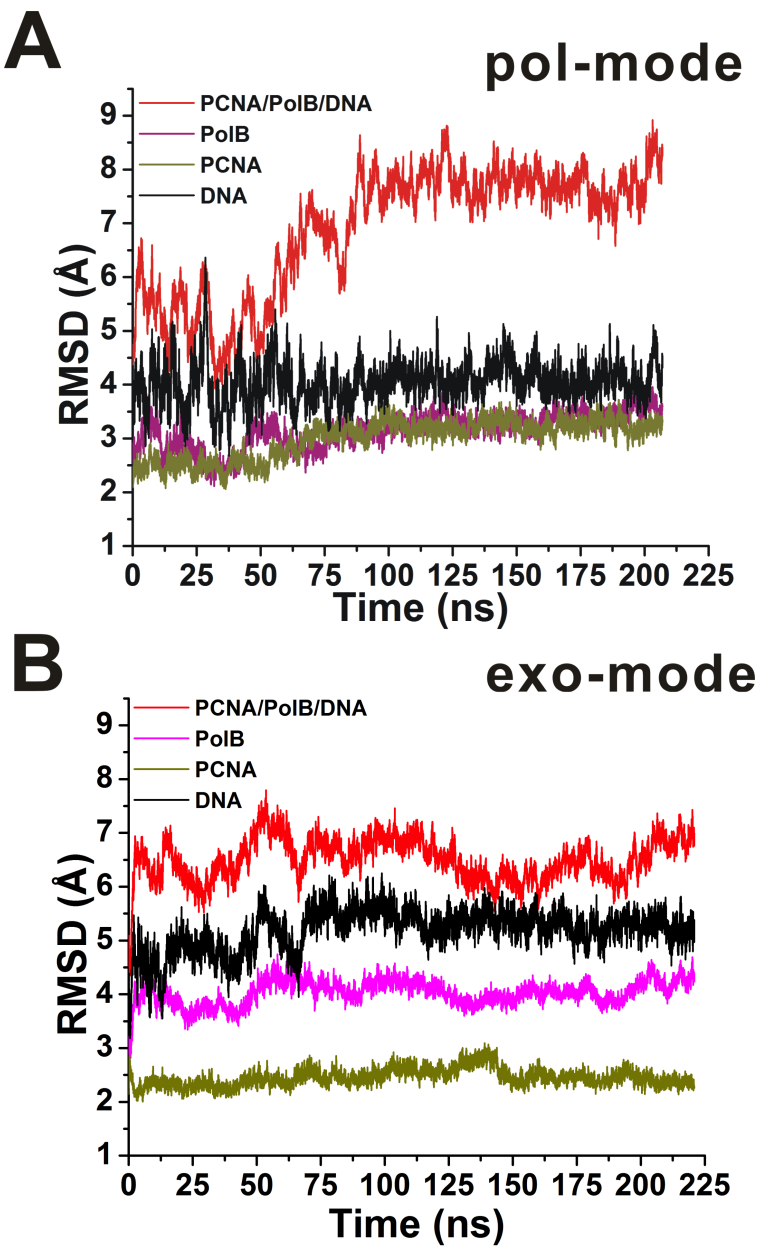

Figure S1. RMSD profiles from the MD simulations of the PolB/PCNA/DNA holoenzyme complex in (A) pol mode; and (B) exo mode.

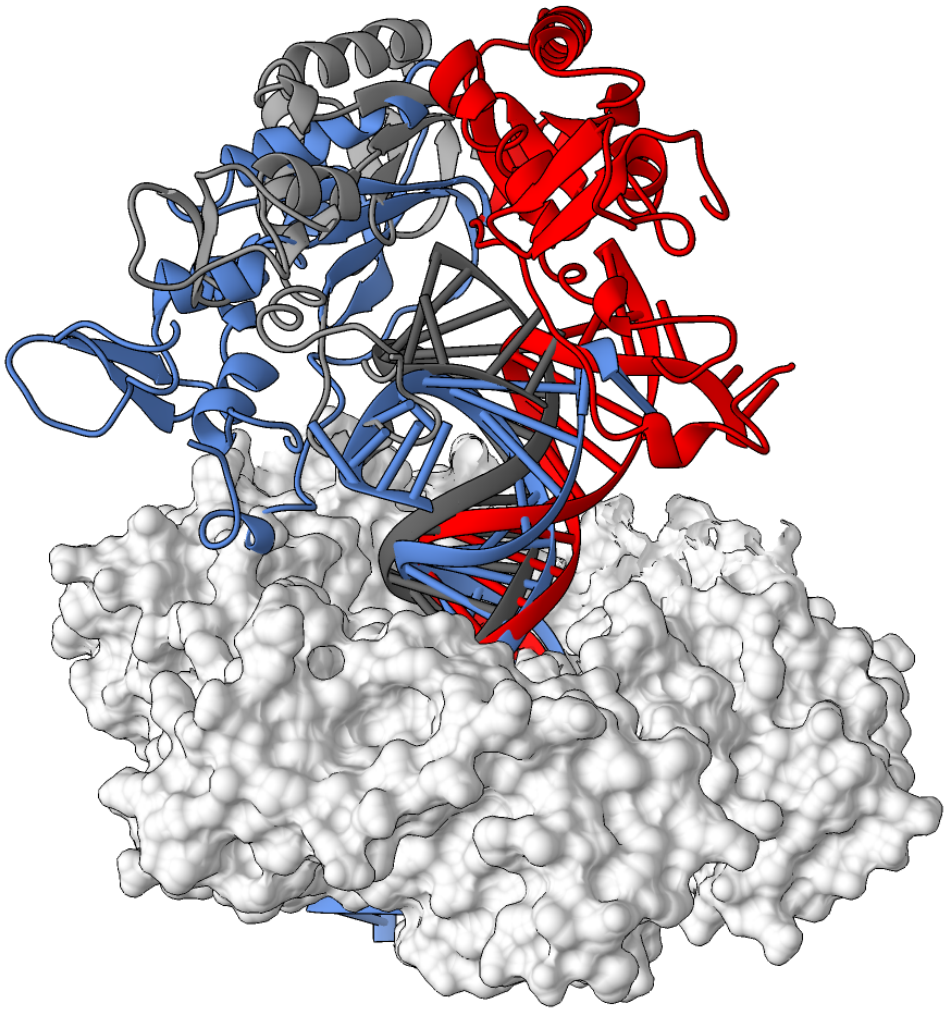

Figure S2. The transition path of the DNA substrate and the rotational motion of the PolB palm domain during the switch from pol to exo mode. The DNA and palm domain are shown in cartoon representation. The PCNA is shown in light gray surface representation. The pathway is represented by overlaid structures selected from the initial (red), middle (dark gray) and final (blue) segment of the TMD trajectory.

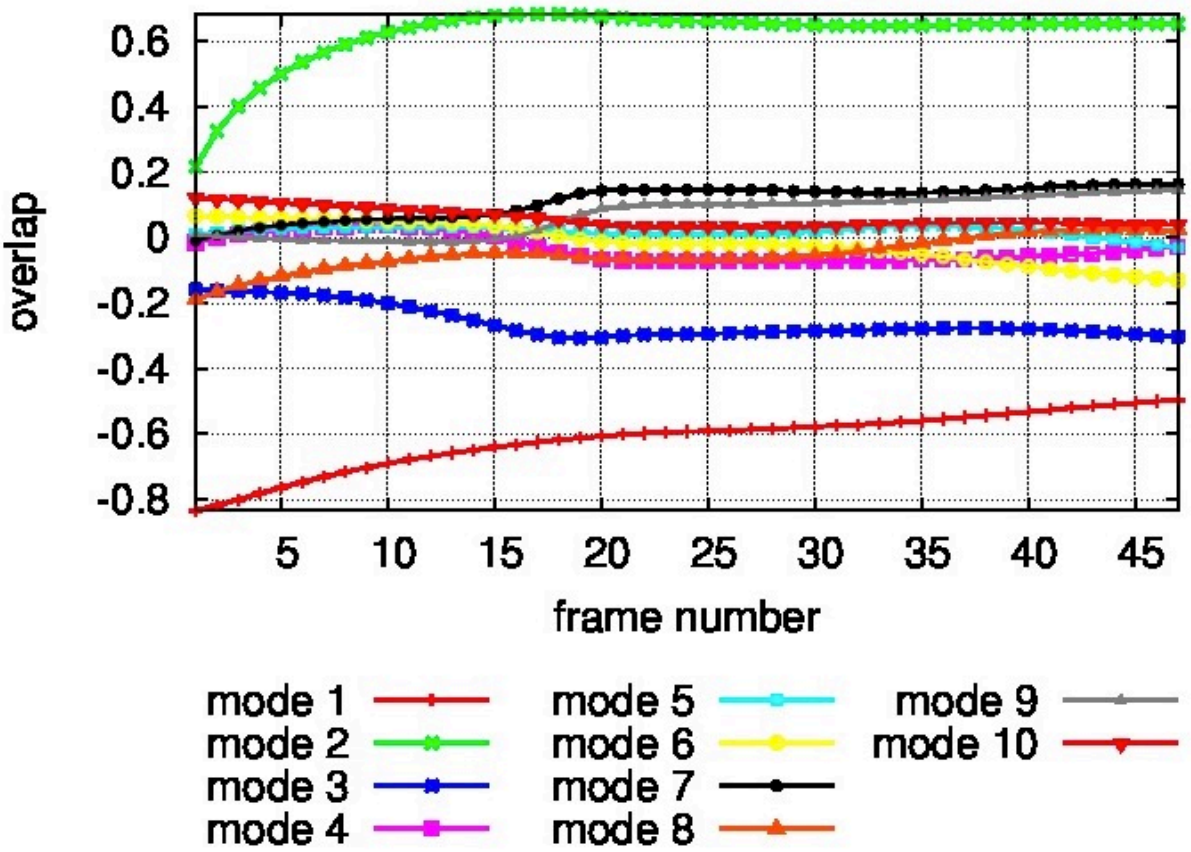

Figure S3. Normal mode contributions to the transition path from pol to exo mode calculated using the path-ENM method. Mode numbering is ordered from low to high frequency. The two lowest normal modes contribute most significantly the transition path.

II. Supplementary Movies

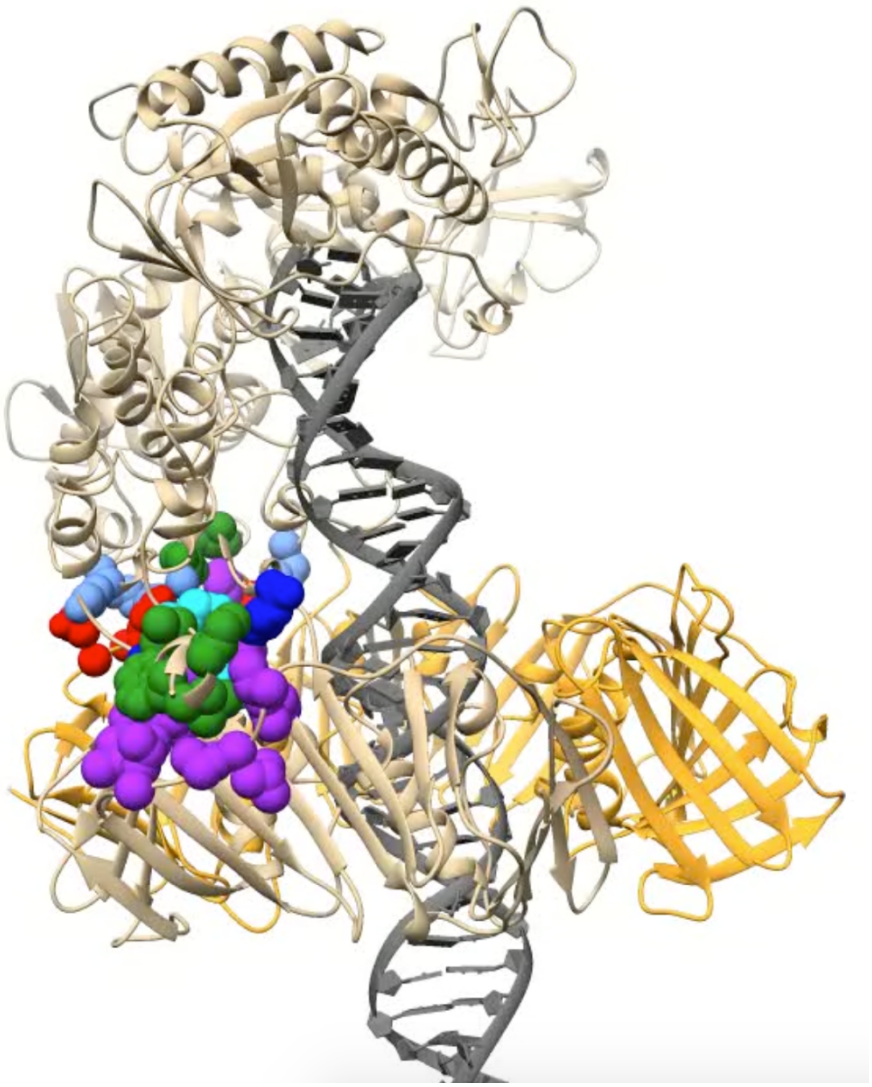

Movie S1. PolB-PCNA contact interfaces in pol mode. Contact residues are explicitly shown in ball and stick representation. Contact types are colored as follows: Salt-bridges in light blue and red; persistent hydrogen bonds (other than salt bridges) in cyan and dark blue; hydrophobic interaction in green and purple.

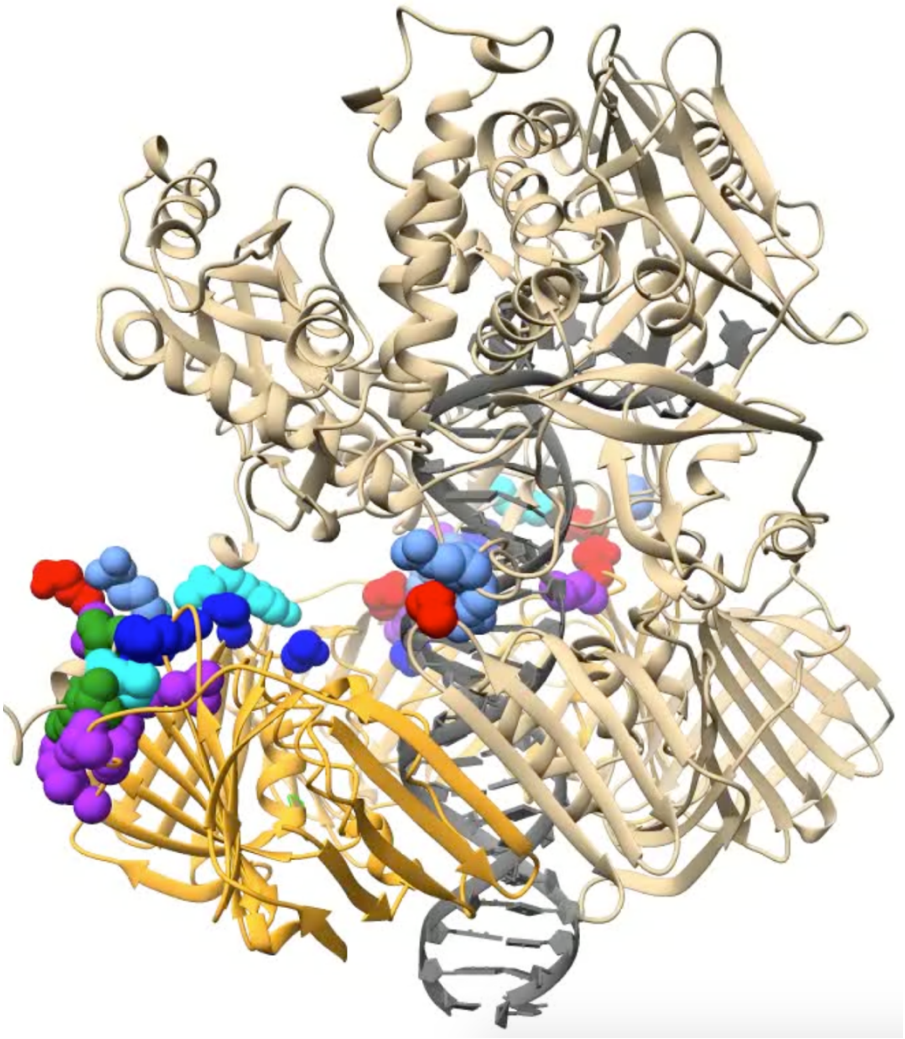

Movie S2. PolB-PCNA contact interfaces in exo mode. Contact residues are explicitly shown in ball and stick representation. Contact types are colored as follows: Salt-bridges in light blue and red; persistent hydrogen bonds (other than salt bridges) in cyan and dark blue; hydrophobic interaction in green and purple.

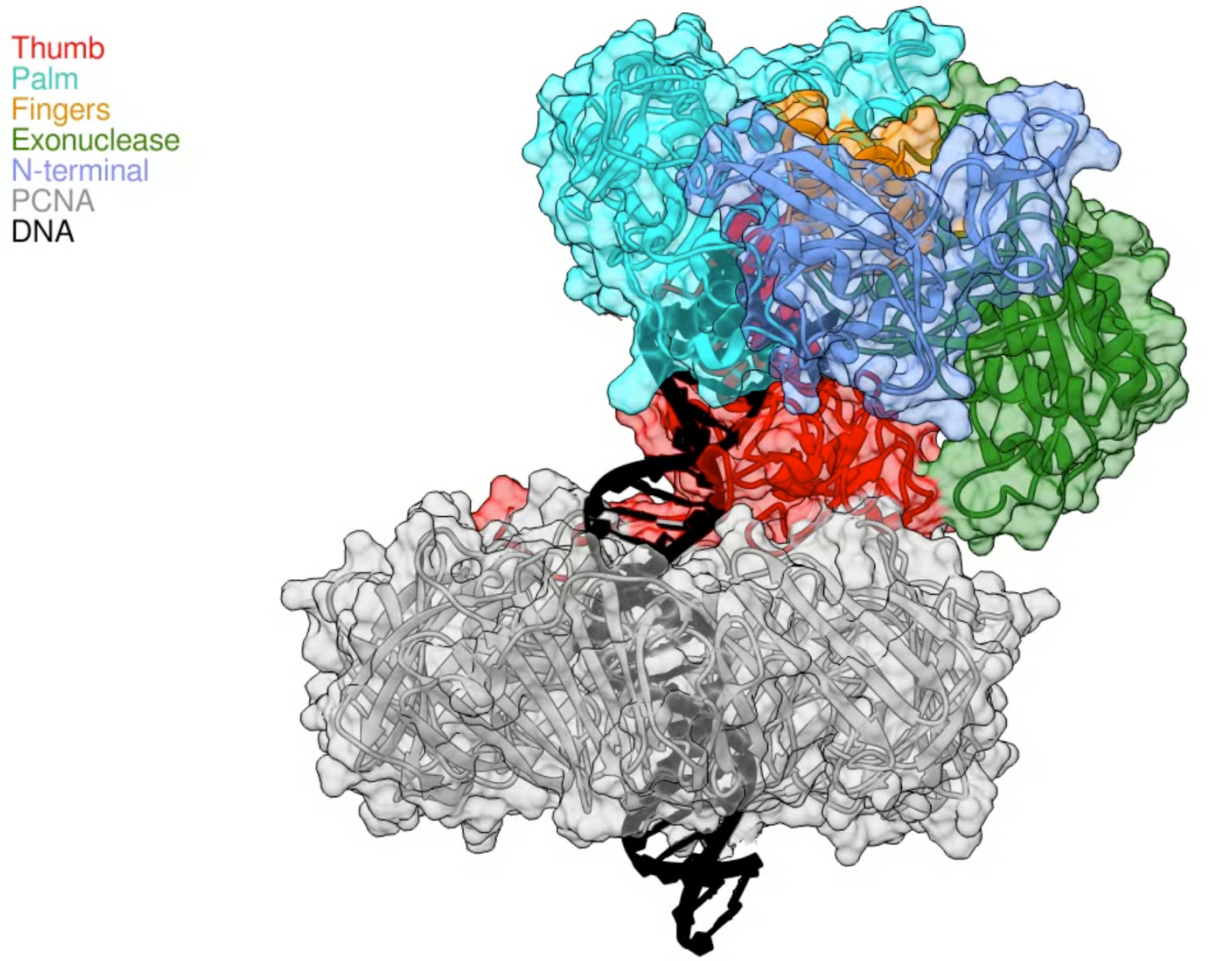

Movie S3. Movie of the conformational switch from pol to exo mode of the PolB holoenzyme complex observed in TMD. PolB domains are colored as follows: N-terminal domain in light blue; exonuclease domain in green; palm domain in cyan; fingers domain in gold and thumb domain in red. PCNA and DNA are shown in grey and black.

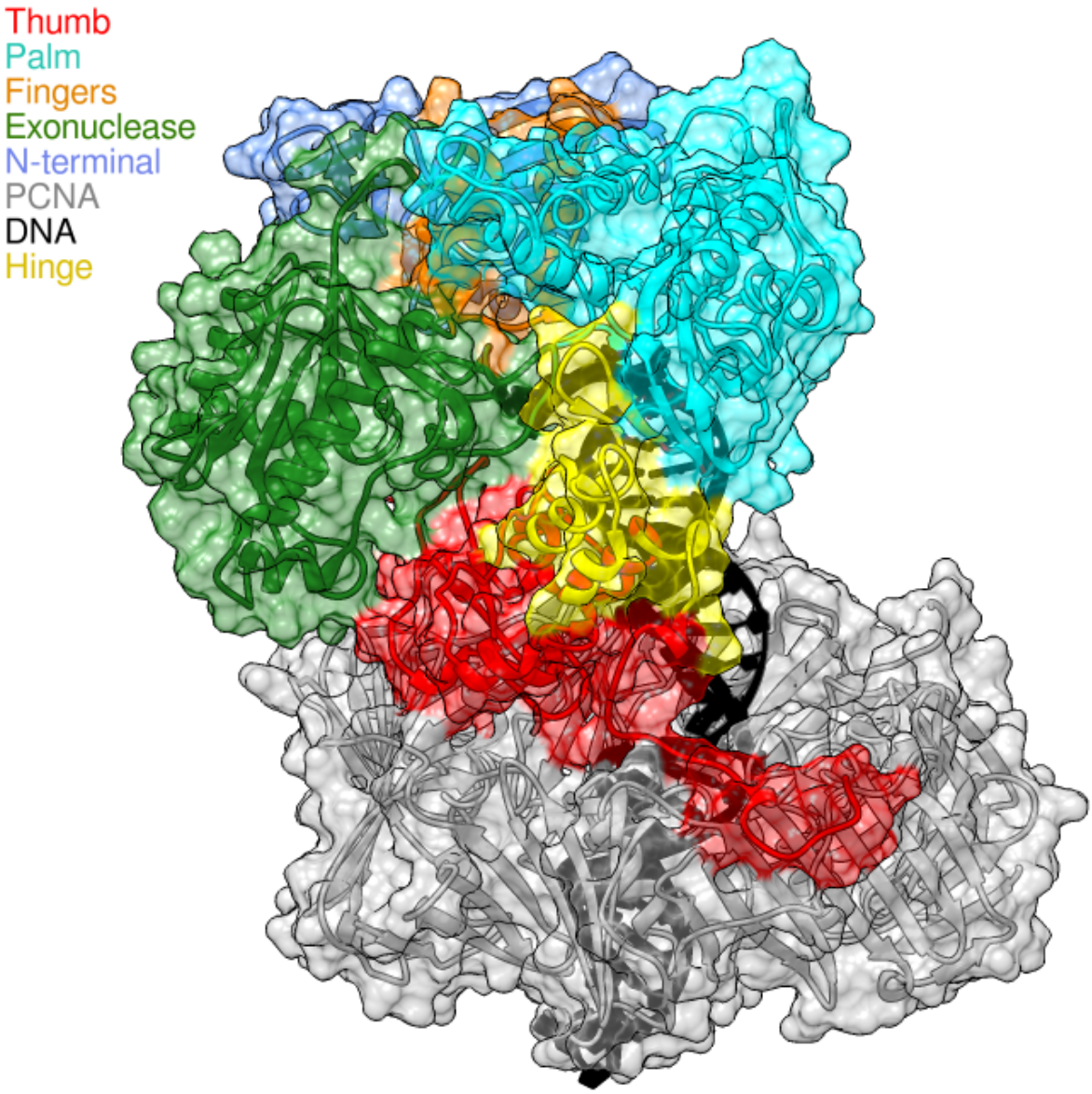

Movie S4. Movie of the conformational switch from pol to exo mode of the PolB holoenzyme complex observed in TMD. PolB domains are colored as follows: N-terminal domain in light blue; exonuclease domain in green; palm domain in cyan; fingers domain in gold and thumb domain in red. PCNA and DNA are shown in grey and black. The hinge region is highlighted in yellow.

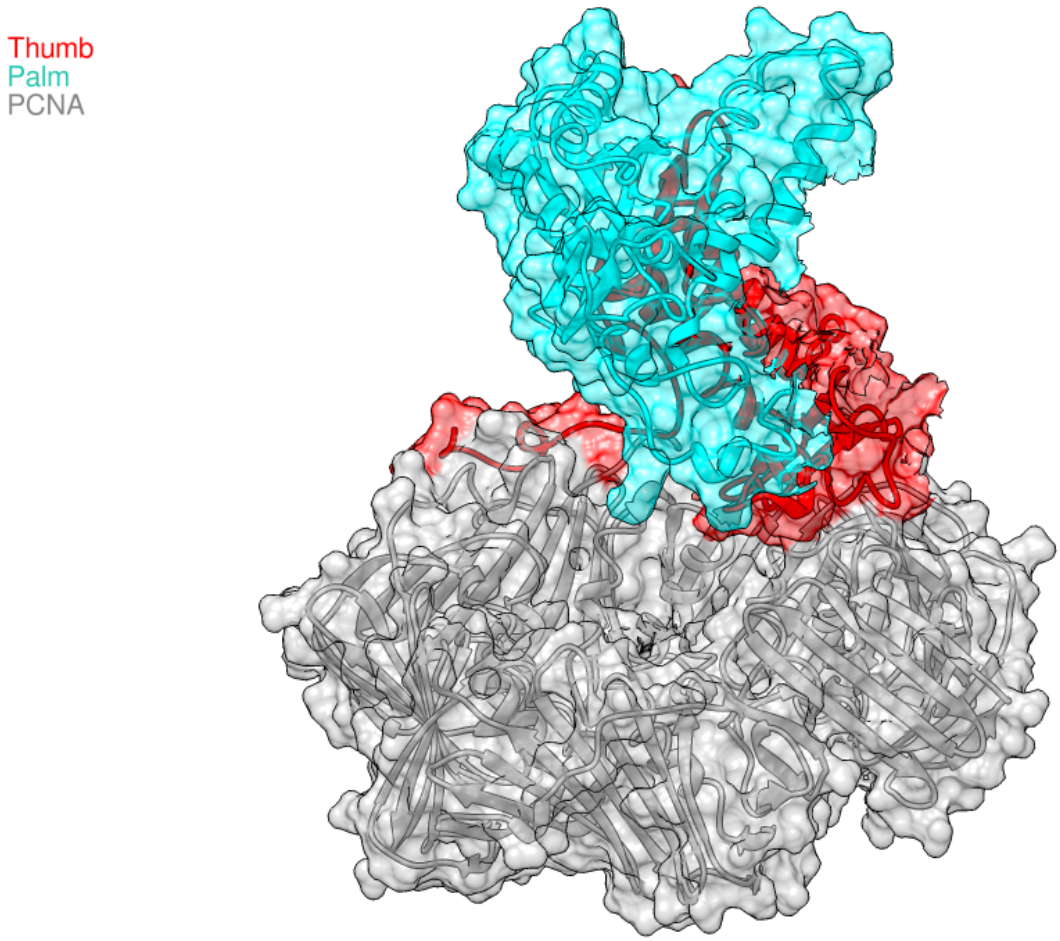

Movie S5. Movie of the conformational transition observed in the targeted MD trajectory. Only the palm and thumb domains of PolB are shown for clarity.

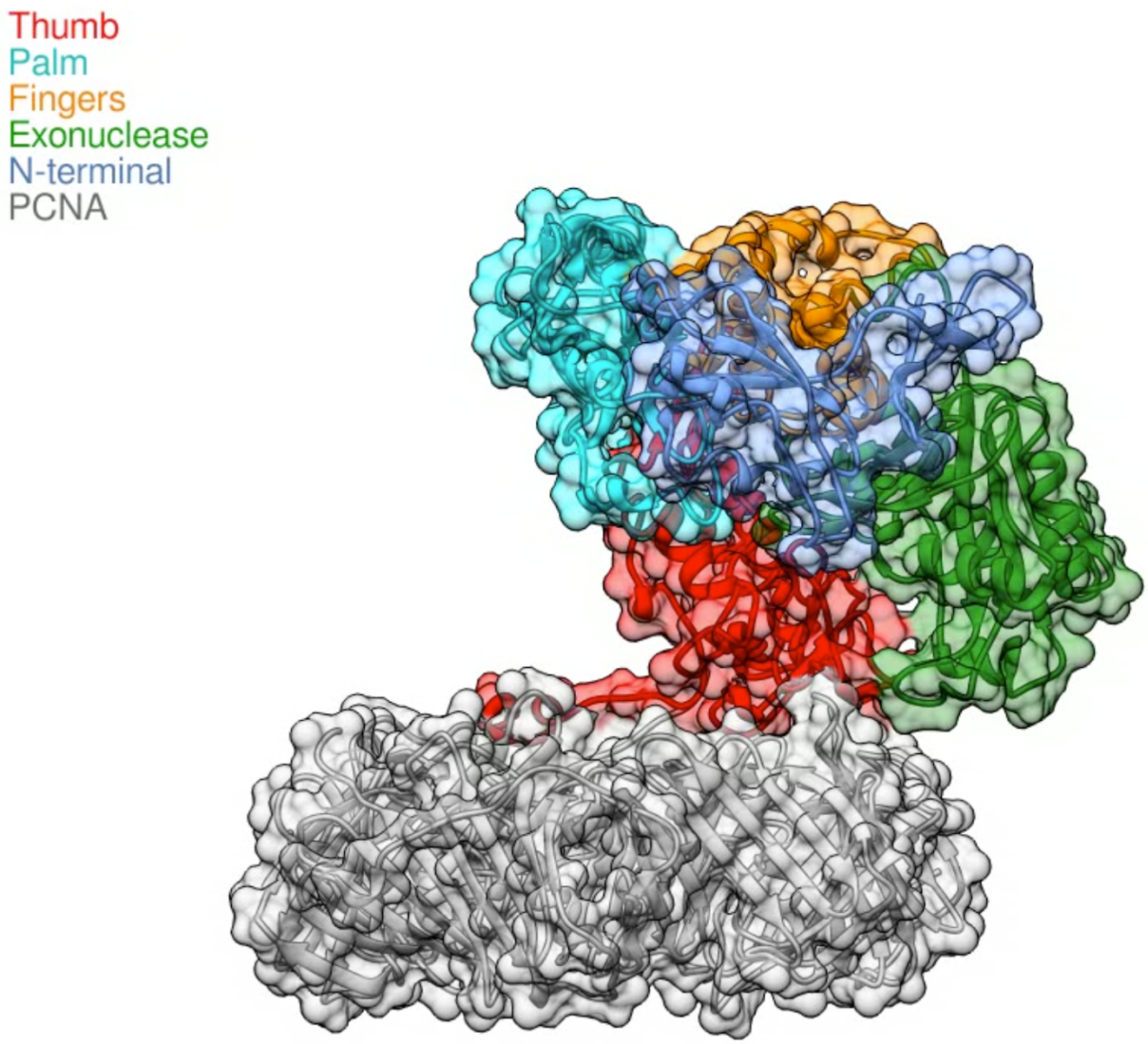

Movie S6. Transition path from pol to exo mode calculated using the path-ENM method. PolB domains are colored as follows: N-terminal domain in light blue; exonuclease domain in green; palm domain in cyan; fingers domain in gold; and thumb domain in red. PCNA is shown in grey. The path is qualitatively similar to the targeted MD trajectory and is comprised primarily of the two lowest normal modes.

III. Supplementary Tables

Table S1. 1D per-residue binding energy decomposition for PolB-PCNA interface residues in pol and exo mode.

pol	ΔG_{GB}[a]	SD[b]	exo	ΔG_{GB}[a]	SD[b]
PolB			**PolB**		
LYS686	-3.74	1.58	ARG382	-5.05	2.69
ARG706	-8.78	2.36	LEU687	-1.14	1.61
ILE716	-1.37	0.37	ALA688	-1.03	0.36
LYS724	-2.35	1.40	LYS690	-2.60	2.43
LYS725	-2.68	1.08	LEU705	-1.08	0.64
GLN763	-2.06	1.27	ARG706	-6.97	1.46
VAL764	-1.07	0.96	ILE716	-1.06	0.56
LEU766	-7.99	0.66	TYR758	-2.97	1.18
TRP769	-4.43	0.70	GLN759	-3.66	1.18
LEU770	-4.13	1.03	THR761	-4.83	1.28
ILE772	-1.62	0.66	ARG762	-8.19	2.36
LYS774	-2.30	2.52	VAL764	-2.87	0.94
PCNA1			LEU766	-7.09	0.69
ARG45	-2.11	0.95	TRP769	-4.09	0.63
VAL46	-2.93	0.50	LEU770	-2.58	0.57
LEU48	-1.09	0.23	**PCNA1**		
VAL123	-4.04	1.72	ARG45	-2.95	2.57
LEU125	-1.08	0.33	LEU48	-1.01	0.29
PRO126	-1.06	0.74	VAL123	-1.49	0.68
LEU128	-1.30	0.40	PRO126	-2.02	0.67
GLU171	-5.28	0.55	LEU128	-1.25	0.54
MET225	-1.18	0.28	SER149	-1.02	1.12
PRO226	-2.08	0.31	ASP153	-3.15	1.37
ALA244	-1.90	0.40	MET225	-1.33	0.37
PRO245	-1.51	0.54	PRO226	-1.91	0.30
ARG246	-3.78	1.28	ALA244	-1.76	0.53
GLU249	-1.66	1.36	PRO245	-2.14	1.04
PCNA3			ARG246	-4.43	1.42
GLU26	-1.59	1.28	VAL247	-5.12	0.65
ASP42	-2.23	1.85	GLU249	-1.57	1.31
PRO43	-2.11	0.48	**PCNA2**		
ASP117	-3.19	1.82	GLU171	-3.16	1.46
GLU119	-2.51	1.53	**PCNA3**		
			SER21	-2.07	0.95
			LEU23	-1.04	0.53
			ILE24	-1.11	1.04
			ASP25	-2.09	1.19
			PRO43	-2.70	0.66
			LEU150	-1.54	0.65
			VAL151	-1.58	0.63
			GLU249	-1.17	2.12

[a]Units: kcal/mol.
[b]Standard Error.

Table S2. 2D pairwise binding energy decomposition for PolB and PCNA interface residues in pol and exo mode.

pol		ΔG_{GB}[a]	SD[b]	exo		ΔG_{GB}[a]	SD[b]
PolB	**PCNA1**			**PolB**	**PCNA1**		
GLY765	ARG45	-1.85	0.35	LEU766	ARG45	-2.87	0.56
LEU766	ARG45	-2.70	0.45	LEU766	VAL46	-1.80	0.31
THR767	ARG45	-1.62	1.11	LEU766	LEU48	-1.27	0.23
GLN763	VAL46	-1.43	0.44	LEU770	VAL123	-1.05	0.65
LEU766	VAL47	-1.05	0.15	LEU770	PRO126	-1.32	0.48
LEU766	LEU48	-1.30	0.19	TRP769	PRO126	-1.21	0.36
ILE772	GLU122	-1.18	0.65	TRP769	LEU128	-1.45	0.60
LEU770	VAL123	-1.28	0.28	TYR758	LEU150	-1.05	0.35
ILE772	VAL123	-1.16	0.34	TYR758	SER152	-4.14	1.20
TRP769	LEU128	-1.30	0.56	GLN759	ASP153	-5.84	1.80
ARG706	GLU171	-8.19	2.47	TYR758	ASP153	-3.28	0.47
ARG706	THR172	-2.52	0.64	GLN759	SER154	-2.03	0.72
TRP769	GLU224	-1.49	0.88	TRP769	MET225	-2.53	0.59
TRP769	MET225	-2.36	0.47	TRP769	PRO226	-2.56	0.30
TRP769	PRO226	-2.61	0.31	LEU766	ALA244	-1.40	0.28
LEU766	LEU242	-1.63	0.37	GLN763	PRO245	-2.01	1.35
LEU766	ALA244	-1.41	0.28	VAL764	PRO245	-2.00	0.63
GLN763	PRO245	-1.15	0.38	TRP769	PRO245	-1.36	0.32
VAL764	PRO245	-1.23	0.93	THR761	ARG246	-4.87	1.84
TRP769	PRO245	-1.61	0.39	GLN763	ARG246	-4.51	2.17
THR761	ARG246	-1.93	0.78	ARG762	ARG246	-3.35	0.61
GLN763	ARG246	-5.51	2.41	VAL764	ARG246	-1.00	0.28
ARG762	VAL247	-3.47	0.96	ARG762	VAL247	-5.41	0.66
PolB	**PCNA3**			THR761	VAL247	-3.11	0.37
ARG706	GLU26	-5.44	3.99	VAL764	VAL247	-1.43	0.38
HIE726	GLU26	-3.08	2.21	**PolB**	**PCNA2**		
LYS686	ASP42	-9.68	3.23	ARG382	VAL151	-1.99	1.61
ILE716	PRO43	-1.39	0.36	ARG382	GLU171	-8.65	4.72
TYR721	PRO43	-1.58	0.46	GLU383	GLU171	-1.53	0.44
LYS686	VAL46	-1.30	0.46	GLU102	LYS196	-1.10	2.42
LYS725	ASP117	-7.24	2.18	**PolB**	**PCNA3**		
LYS724	GLU119	-9.87	2.89	ARG706	SER21	-4.52	1.46
LYS724	GLU120	-1.59	1.13	ARG706	LEU23	-1.34	0.38
				ARG706	ILE24	-1.89	0.51
				ARG706	ASP25	-13.27	1.46
				LYS727	PRO43	-1.93	0.42
				LYS725	PRO43	-1.52	0.64
				HIE726	PRO43	-1.13	0.41
				LYS685	LEU150	-1.83	1.09
				ASN713	LEU150	-1.22	0.80
				LYS686	LEU150	-1.19	0.56
				LYS685	VAL151	-1.83	0.58
				LYS690	ASP153	-5.12	5.09
				ALA688	GLU171	-1.00	0.66
				LYS690	GLU249	-7.48	4.75

[a] Unit: kcal/mol.
[b] Standard Error.

IV. Supplementary atomic models

Model S1. Model of PolB holoenzyme in polymerization mode (pol_polb.pdb).
Model S2. Model of PolB holoenzyme in exonuclease mode (exo_polb.pdb).

V. Supplementary references

1. Case, D. A.; Darden, T. A.; Cheatham III, T. E.; Simmerling, C. L.; Wang, J.-M.; Duke, R. E.; Luo, R.; Merz, K. M.; Pearlman, D. A.; Crowley, M.; Walker, R. C.; Zhang, W.; Wang, B.; Hayik, S.; Roitberg, A.; Seabra, G.; Wong, K. F.; Paesani, F.; Wu, X.; Brozell, S.; Tsui, V.; Gohlke,H.; Yang, L.-J.; Tan, C.-H.; Mongan, J.; Hornak, V.; Cui, G.-L.; Beroza, P.; Mathews, D. H.; Schafmeister, C.; Ross, W. S.; Kollman, P. A. Amber 9. *University of California, San Francisco* **2006**.